

**SURVIVAL OF LONGITUDINAL HOLES IN THE PS BOOSTER
COASTING PROTON BEAM**

A. Blas, S. Hancock, S. Koscielniak, M. Lindroos

Abstract

The purpose of the 24th November 1999 MDs was to investigate the survival of holes originally in the linac beam after injection into the Booster, and the effect of cleaning sweeps upon them and the beam momentum distribution. Further, investigation was made of holes deliberately introduced into the coasting beam by high harmonic empty bucket deposition. A number of different schemes for the clearing sweep were tried. Also, the influence of beam intensity on these phenomena was studied.

1 Introduction

During the MDs proceeding the 24th November, particularly those on 16th and 18th November, a number of minor problems became evident in the attempts to record the evolution of “linac bubbles” and high-harmonic empty bucket holes. Firstly, it was very unfortunate when we were trying to diagnose “bubbles”, that the graphical primitive used by the “tomoscope” to generate a grey scale was itself a small circle. Secondly, the acquisition triggering of the tomoscope has to maintain synchronism with the revolution frequency of the bubbles or holes, else the displays become confusing. The first problem was circumvented by writing the tomoscope data to file and then processing it off-line with the puissance of “Mathematica”. The second problem can only be avoided by careful and time consuming adjustment of the RF by trial and error. Both these improvements in data acquisition and processing were available for the 24th November MD. The Shottky scans were acquired with the HP 89410A signal analyzer tuned to the 6th harmonic of the revolution frequency.

1.1 Mathematica notebooks

Multiple beam longitudinal profile data was acquired using the “Tomoscope” software and then processed in various “Mathematica” notebooks with titles:

“/usr16/mafia/Nov99MD/waterfall-holes.nb” and

“/usr16/mafia/Nov99MD/waterfall-steve0,1,2,3,4,5.nb”.

The “spectrograms” were made in “/usr16/mafia/Nov99MD/waterfall-FT2.nb”.

1.2 Tomoscope triggering

The waterfall display of beam current within a single turn versus turn number, known at CERN PS as the “tomoscope”, displays “phase at arrival” (at the pick-up) information about local beam intensity features. The turn number and acquisition triggering is taken from the fundamental frequency which may well not be the beam revolution frequency. Consider now a coasting beam (i.e. no cavity voltage but nevertheless a low-level rf reference signal). A constant offset between these two frequencies produces a linear movement versus turns of any “phase-feature” in the beam. A ramped offset between beam and reference frequencies implies that phase accumulates quadratically with time, and will give rise to parabolic movement versus time of any beam intensity feature. Hence, to make meaningful (and easy to interpret) tomoscope measurements on a coasting beam implies that (i) the reference frequency must be constant, and (ii) reference and beam-hole revolution frequencies should be equal. Unfortunately, in previous MDs, we inherited an RF program (from a beam cycle intended for another purpose) that is a sequence of ramps; and so neither of these conditions were met in previous studies of coasting beams and space-charge stabilized bubbles. In the present MD we would be more careful and so set the RF equal to the revolution frequency of the holes.

1.3 General Plan

The general plan of the observations was starting from a complicated triple-sweep clearing schema to progressively simplify the clearing program, and at each stage of this simplification study the behaviour as a function of injected beam intensity.

2 C02,C04,C16 all OFF

First we review the behaviour with no clearing sweep, but as a function of the injected beam intensity. Experiments were performed on an MEFLAT cycle at 50 MeV with injection occurring at 275 ms of the C-train.

2.1 3 turns injected, 2.3E12ppp, inject @ C-train=275ms

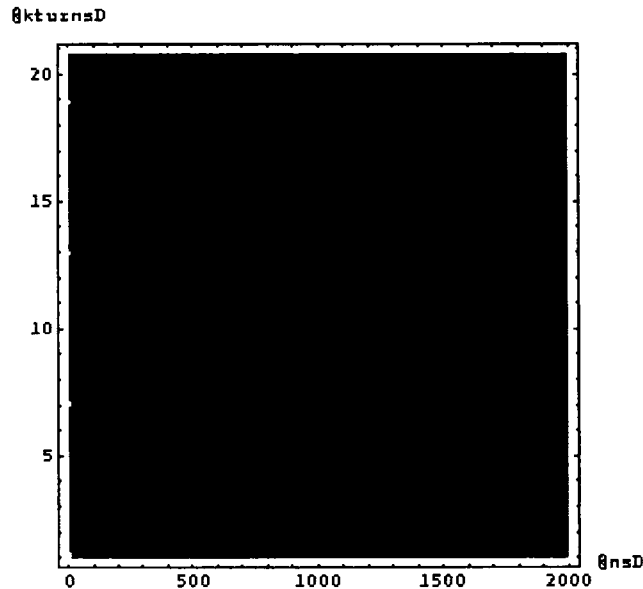


Figure 1: C16 OFF, 30 turns/trace, 100 traces, start @ inject+8ms, span =5 ms, 20mV/div .

The horizontal span of the plot is 1.2 turns. The grey scale gives a visual depiction of the relative particle density; black corresponds to the most dense, and white to the most rarified. Evidently, the off-white diagonal tracks are sub-structure from the linac beam that survives the injection process and circulates for several milliseconds thereafter.

Date: 24.11.99 Time: 13:21

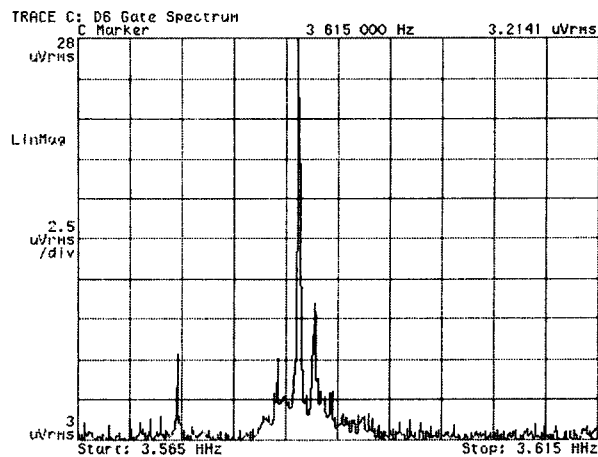


Figure 2: Schottky scan, C16 Off, 3 turns injected .

The Schottky spectrum, Figure 2, is annotated with “summer time” which is an hour in advance of “day-light saving” and so the local time was really 12:21 pm. This information is useful in marrying the Schottky data with the tomoscope data. The very tall and narrow spikes appearing in the spectrum are most likely “coherent signals” rather than very high particle densities.

Later the final value of GSRPOS GFA was fine tuned so that 0.9 injected turns debunches symmetrically. In this way the apparent sideways drifting of the tracks was slowed down, enabling the time-span to be increased from 5 ms to 33.3 ms. One may obtain a little more contrast in the density plots by removing the first few profiles which contain the last vestiges of h=1 beam structure (from the injection process).

2.2 1 turn injected, 1.0E12ppp, inject @ C-train= 275ms

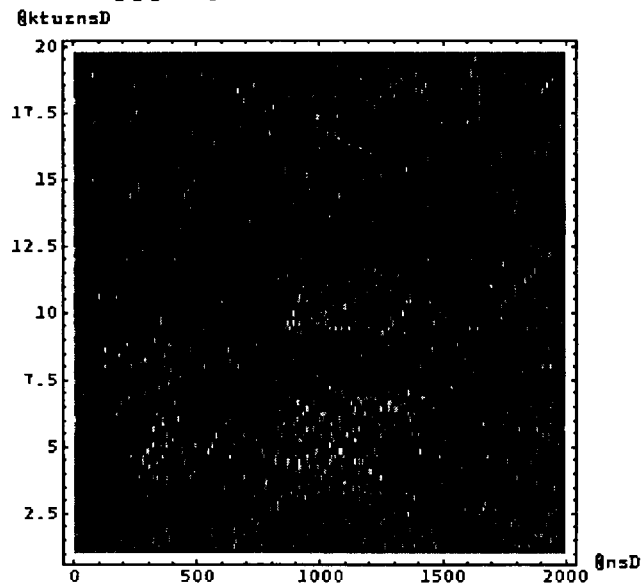


Figure 3: C16 OFF, 200 turns/trace, 95 traces, start @ inject+1.6ms, span =31.7ms, 2mV/div .

To a particle physicist accustomed to looking at tracks in a bubble chamber or photographic emulsion, the holes or “bubbles” in the linac beam leave clear coherent traces which span more than 30 ms.

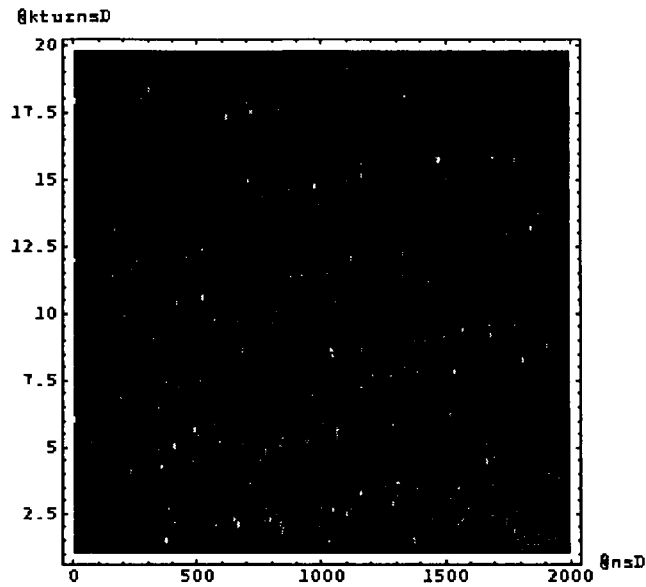


Figure 4: C16 OFF, 200 turns/trace, 95 traces, start @ inject+1.6ms, span =31.7ms, 5 mV/div .

A linac beam hole persists as a sinuous grey-white track running from bottom-centre to top-left of Figure 4. There is also faint evidence for h=1 structure as a wrapped diagonal line from bottom-left to top-right. 2 turns injected, 1.6E12ppp, inject @ C-train= 275ms.

Date: 24.11.99 Time: 13:51

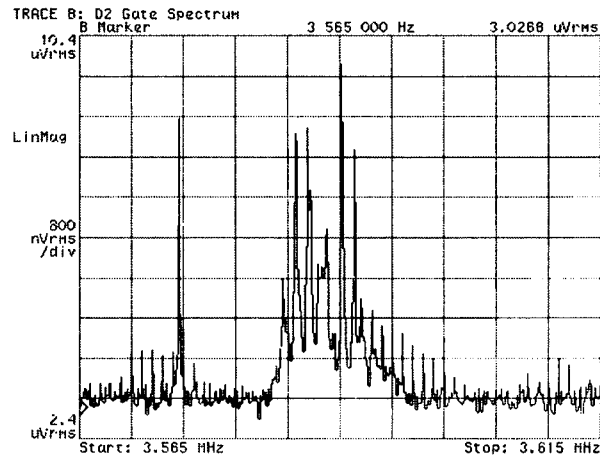


Figure 5: Schottky scan; C16 Off, 2 turns injected .

The Schottky scan, Figure 5, probably consists of several small coherent signals superposed on the incoherent background signal and is probably more indicative of the beam distribution than Figure 2.

2.3 3 turns injected, 2.4E12ppp, inject @ C-train= 275ms

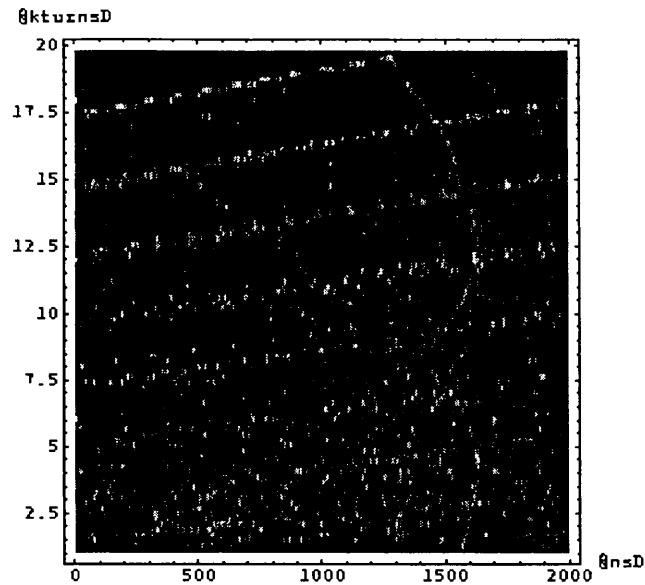


Figure 6: C16 OFF, 200 turns/trace, 95 traces, start @ inject+1.6ms, span =31.7ms, 5 mV/div .

There are several linac bubbles present as evidenced by the two main parabolic tracks. More careful inspection yields the rightmost parabola to be the confluence of three initial tracks. Again there is evidence of $h=1$ structure wrapping across the waterfall density plot. This is confirmed by Fourier analysis of each turn which shows strong $h=0$ and $h=1$ components, and very weak but growing $h=3,4$ components; all other Fourier components are probably “noise”.

Date: 24.11.99 Time: 13:58

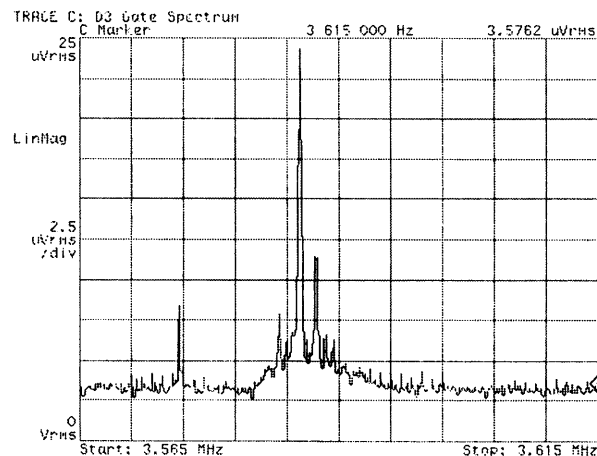


Figure 7: Schottky scan; C16 Off; 3 turns injected .

The Schottky scan, Figure 7 (which is very similar to Figure 2), has a stronger peak than in Figure 5 (2 turns injected) which might suggest the coherent signal is enhanced by space charge.

2.4 4 turns injected, 3.6E12ppp, inject @ C-train= 275ms

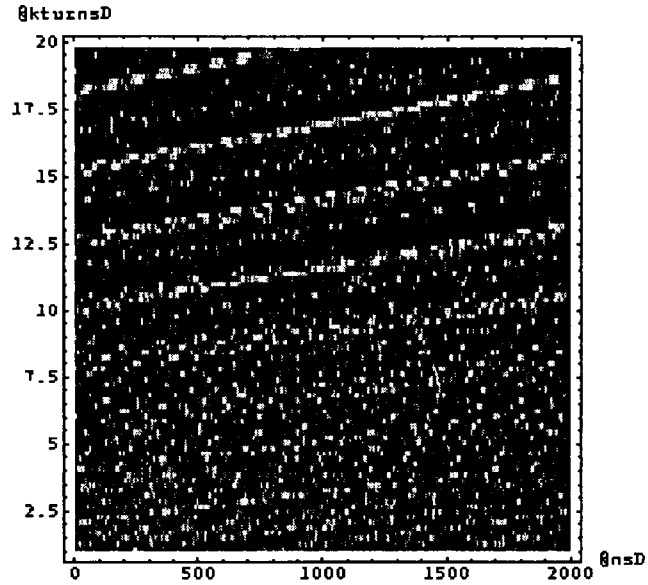


Figure 8: C16 OFF, 200 turns/trace, 95 traces, start @ inject+1.6ms, span =31.7ms, 5 mV/div, Δf GFA=0.0V .

There is even stronger evidence of $h=1$ structure in Figure 8, and its revolution frequency continues to depart from the reference sampling RF. Fourier analysis, Figure 9, reveals along with $h=0,1$ harmonics, weak but sporadically growing $h=2,3,4$ components. The spectrogram is similar to Figure 12.

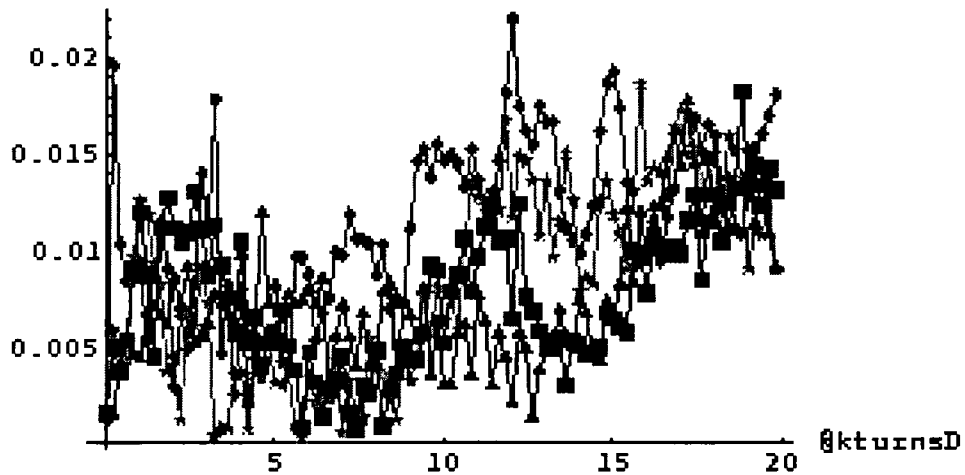


Figure 9: red diamond $h=1$, green star $h=2$, blue square $h=3$, black triangle $h=4$, Fourier components .

The spike in the Schottky scan, Figure 10, is undoubtedly a coherent signal which is enhanced by a collective effect (the intensity has been raised compared with Figure 7).

Date: 24.11.99 Time: 14:09

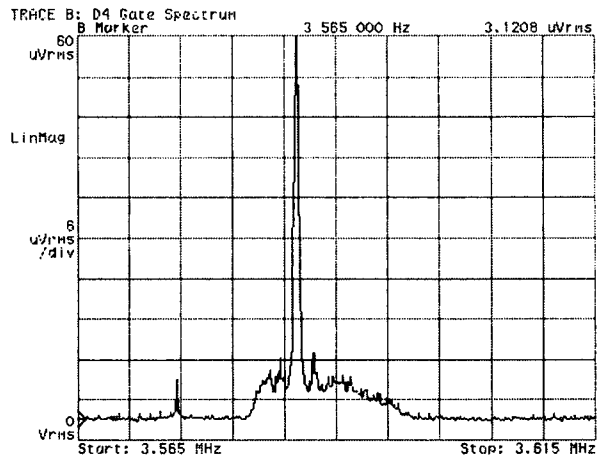


Figure 10: Schottky scan; C16 Off, 4 turns injected .

GSRPOS controls the low-level RF signal which is used to trigger the turn-by-turn of beam current profiles. The RPOS GFA was set to -0.5 volt so as to remove the diagonal drift (of the $h=1$ structure) from the waterfall display. In interpreting the resulting plot, one must be mindful that the horizontal span is 1.2 turns. What we now see (Figure 11) are a number of beam holes several of which collide and pass over or through one another; and perhaps one pair that coalesce.

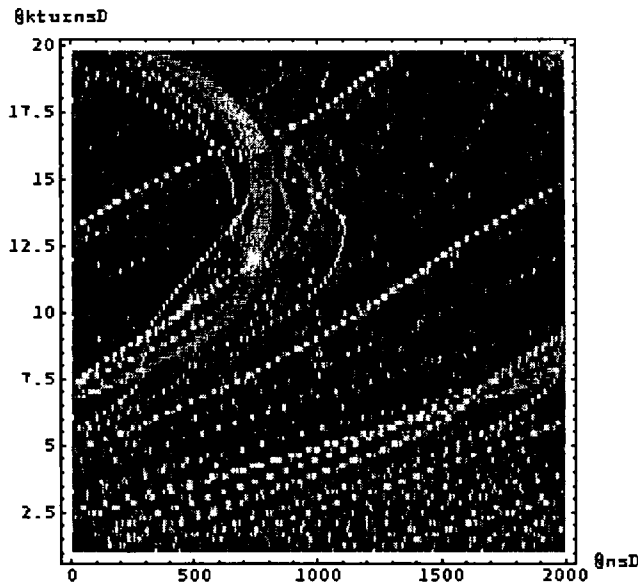


Figure 11: C16 OFF, 200 turns/trace, 95 traces, start @ inject+1.6ms, span =31.7ms, 5 mV/div, Δf GFA = $-0.5V$, 4 injected turns .

The dominant signal in the spectrum of Figure 10 is undoubtedly associated with the strong coherent $h=1$ feature in Figure 11. The grey or colourscale depiction of the Fourier content within a single trace versus many consecutive traces is called a "spectrogram" and shows (Figure 12) strong $h=0,1$ harmonics along with weak but sporadically growing $h=2,3,4$ components.

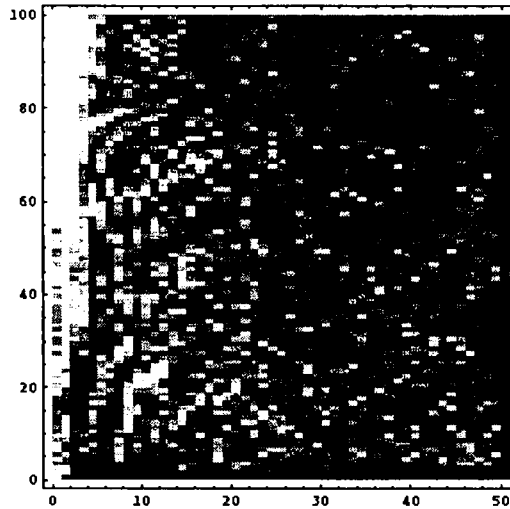


Figure 12: “Spectrogram” or Fourier components (abscissa) versus profile number (ordinate) corresponding to Figure 11 .

2.5 5 turns injected, 4.8E12ppp, inject @ C-train= 275ms

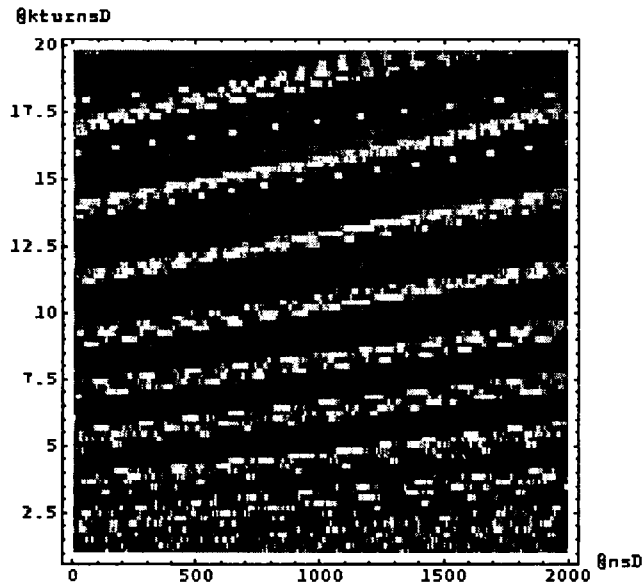


Figure 13: C16 OFF, 200 turns/trace, 95 traces, start @ inject+1.6ms, span =31.7ms, Δf GFA=0.0V .

With GSRPOS set to zero, again one sees $h=1$ structure whose departure from the reference sampling RF progressively diminishes. The spectrogram (similar to Figure 12) reveals strong $h=1$ along with $h=0,2$ and weak (not growing) $h=3,4$ components. The Schottky scan, Figure 14, reveals an even stronger coherent signal (c.f. Figure 10) which can be attributed to the greater intensity and collective effect.

Date: 24.11.99 Time: 14:18

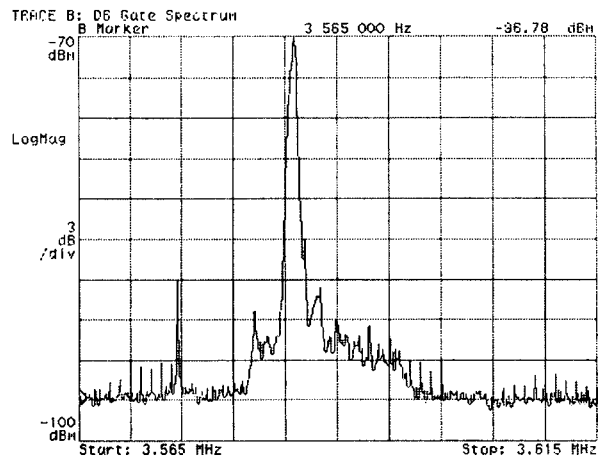


Figure 14: Schottky scan, C16 Off, 5 turns injected .

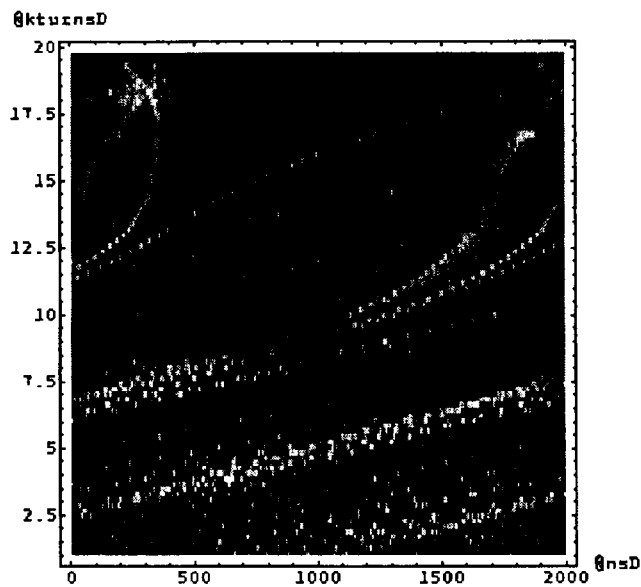


Figure 15: C16 OFF, 200 turns/trace, 95 traces, start @ inject+1.6ms, span =31.7ms, 5 mV/div, Δf GFA=-0.5V, 5 injected turns .

After GSRPOS GFA is restored to = -0.5V, the drift of h=1 structure is slowed down revealing a cluster of holes (Figure 15) that initially move as one entity. Later some parts of the cluster separate due to their differing momenta, while one hole debunches. The spectrogram indicates strong h=1 along with h=0,2 and weak h=3,4 components (not growing); all other components are “noise”.

2.6 8 turns injected, 5.8E12ppp, inject @ C-train= 275ms

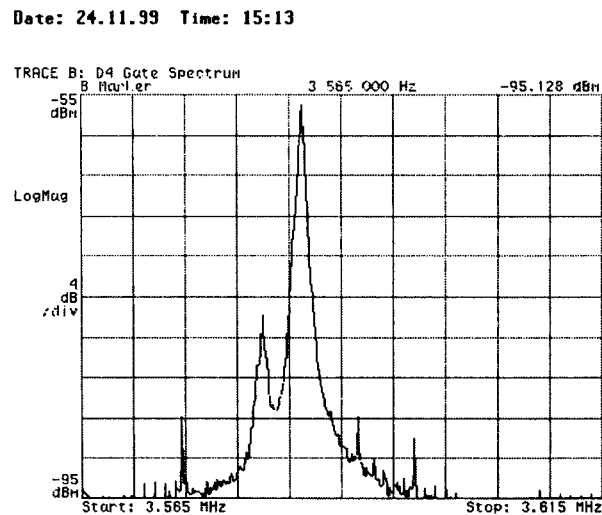


Figure 16: Schottky scan, C16 Off, from TC16OF38.dat .

The spectrum in Figure 16 is reminiscent of that obtained in the 17th November MD with 10 injected turns.

3 C02,C04 OFF, C16 ON, 3 clearing sweeps, h=20

The C16 cavity is used to perform “clearing sweeps” by the passage of high harmonic empty buckets through/across the beam momentum distribution. The sweeps may be followed by an empty bucket deposition. The utility of the “cleaning sweep” lies in the fact that it seems to eliminate some of the sub-structure present from the linac beam.

3.1 3 Clearing sweeps & bucket deposit, 3 turns injected, 2.4E12ppp

C16 cavity GFA=3V, hence gap voltage = 3 kV. GSRPOS GFA =-4.5V @ injection, sweeps up to +4.5V in 2ms, sweeps down to -4.5V in 2ms, sweeps up to +4.5V in 2ms, sweeps down to 0.0V in 1ms at which time the cavity voltage is reduced to zero. The process is completed in 7 ms. The effect of the final bucket deposition is evident in the 24 black and white stripes at the bottom of Figure 17; however, the harmonic number is 20 and the span of the plot is 1.2 turns.

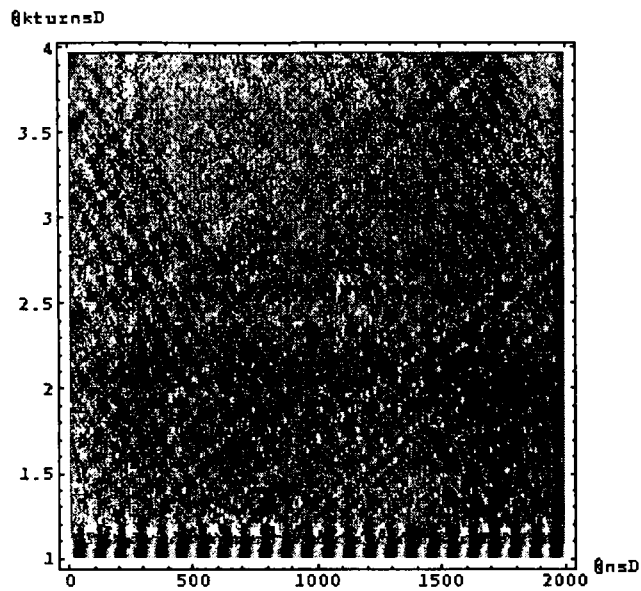


Figure 17: C16 ON 30 turns/trace, 100 traces, start @ inject+8ms, span =5 ms, 20mV/div .

One may obtain a little more contrast by removing the last vestiges of $h=20$ bunched beam in the first few profiles, as has been effected in figure 3. The diagonal lines (of which there are approx 24) sloping from bottom-right to top-left are most likely vestiges of the holes created by the empty buckets. Three injected turns were used, Figure 18.

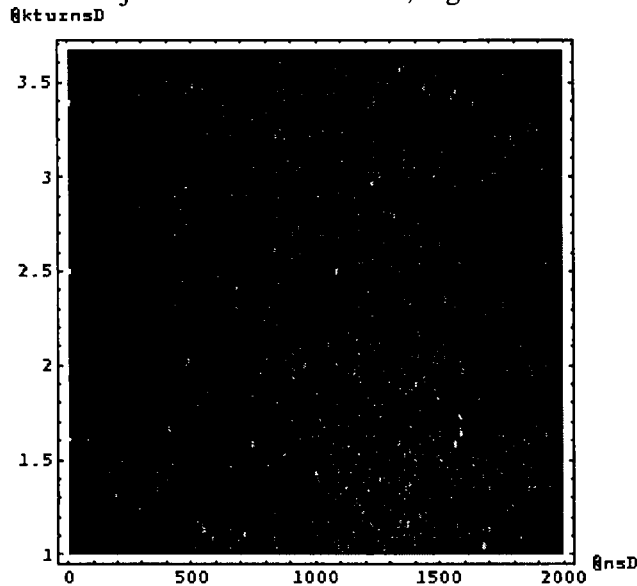


Figure 18: C16 ON 30 turns/trace, 90 traces, start @ inject+8.5ms, span =4.5 ms, 20mV/div .

Date: 24.11.99 Time: 13:25

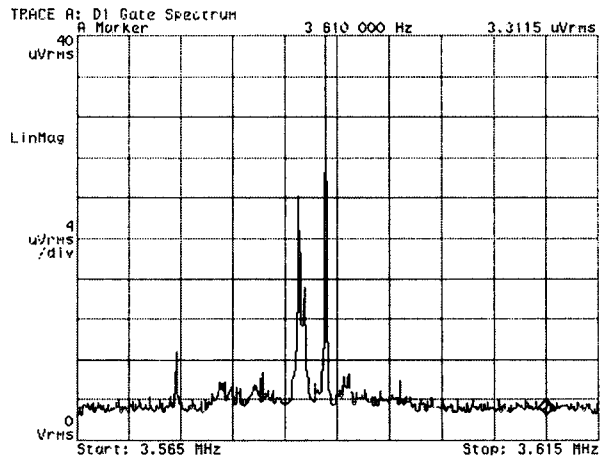


Figure 19: Schottky scan; 3 clearing sweeps, bucket deposit, 3 turns injected .

It appears, Figure 19, that two coherent spikes/signals survive the clearing sweeps. However, they might be the “notch” left over from the bucket deposit – if coherent signals are associated with the notch.

3.2 3 Clearing sweeps but no bucket deposit, 3 turns injected, 2.4E12ppp

We made a slight variation in which there were 3 clearing sweeps as before, but no final deposition of empty buckets. The C16 cavity programs are given in Figure 20.

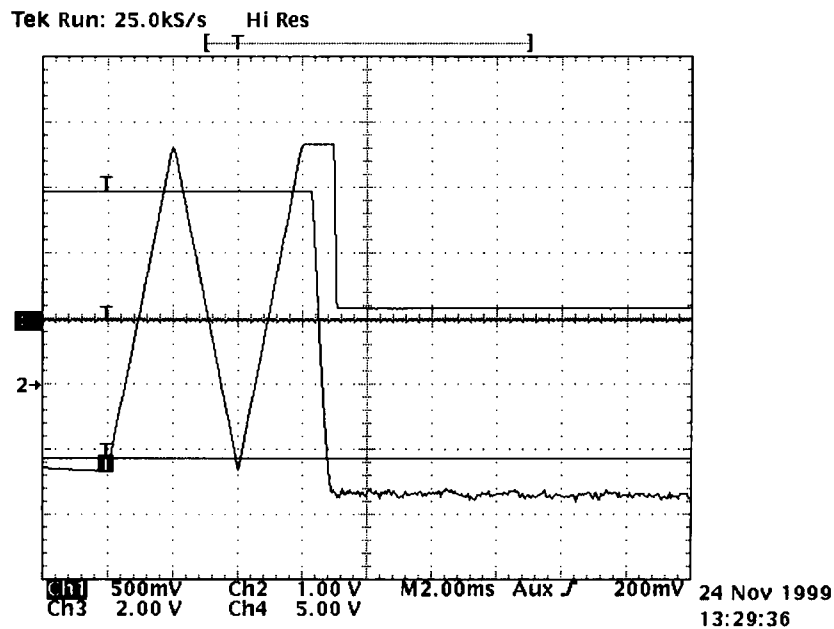


Figure 20: C16 cavity frequency (channel #3) and voltage (dB channel #1) laws .

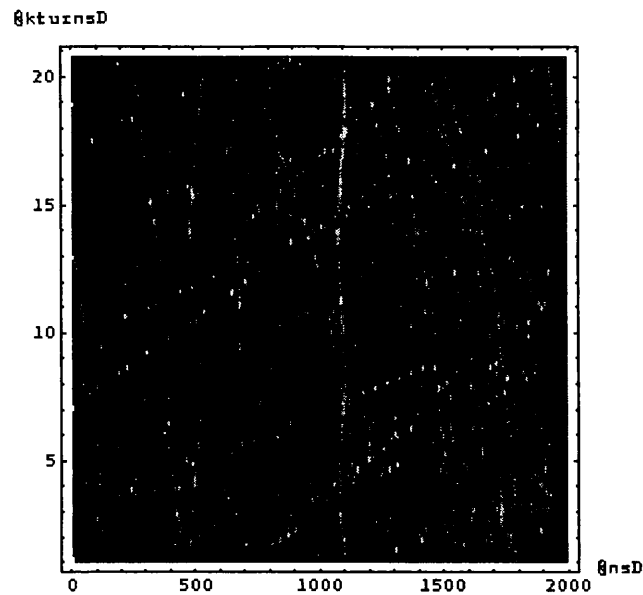


Figure 21: C16 ON 30 turns/trace, 100 traces, start @ inject+8ms, span =5 ms, 20mV/div .

Certainly (Figure 21) the regular array (Figure 17) of $h=20$ density perturbations has disappeared. Nevertheless, there are still holes surviving; and it is difficult to say if these are linac holes or coherent structure surviving from the clearing sweeps. Three injected turns were used, Figure 21.

Date: 24.11.99 Time: 13:31

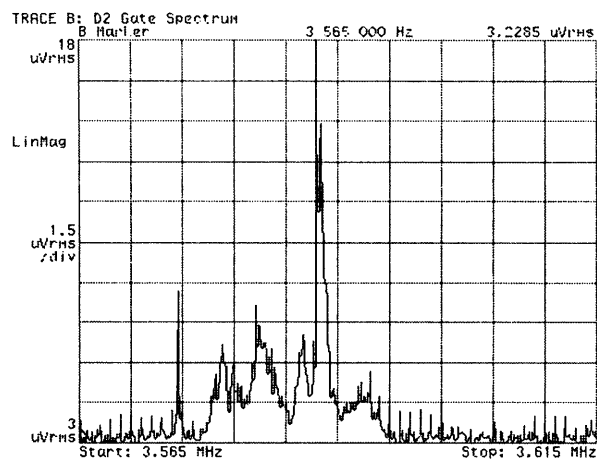


Figure 22: Schottky scan; 3 clearing sweeps, no bucket deposit; 3 turns injected .

The scan immediately above differs from Figure 19, but it is hard to interpret the differences.

3.3 Evidence of 200 MHz linac structure?

Amidst this plethora of structure in the “tomoscope” displays, it is worth asking could any of this have come from empty or partially filled RF buckets of the 200 MHz linac beam. To answer this question, one must sharpen the resolution to 2 ns or better. The resolution of the Tektronix scope is 4 ns, so one may expect 200 MHz structure to occupy 2 bins, giving an appearance of up to 8 ns width. The Figure 23 below shows a horizontal zoom of tomoscope data acquired under conditions corresponding to Figure 15: the C16 cavity is off and 5 turns

were injected. In this example, the horizontal axis has been expanded to zoom in on two streaks that cross the figure diagonally. Unfortunately, the diagonal motion has the effect of broadening the streak to about 40 ns.

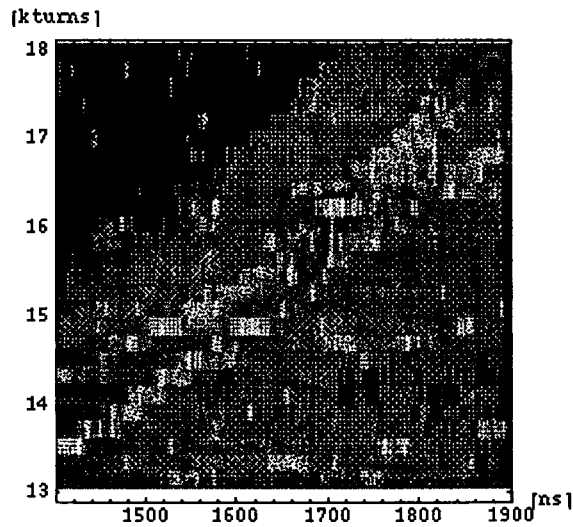


Figure 23: zoom to show scale of structure; C16 off, 5 turns injected, start @ C-train =275 ms, 100 traces, 200 turns/trace, Δf GFA=-0.5V.

In Figure 24 below, which is derived from Figure 21, there is a vertical streak occurring around 1100 ns; and this is a better candidate for a width measurement. The streak appears about 10 ns wide, which given the resolution and allowing for some broadening due to momentum spread, is compatible with 200 MHz.

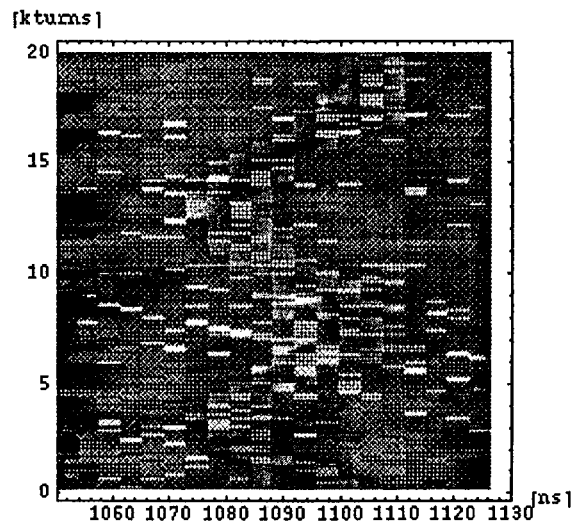


Figure 24: zoom of earlier figure to show 10 ns structure, C16 clearing sweep but no bucket deposit; 3 turns injected; span =5 ms.

4 C02,C04 OFF, C16 ON, single clearing sweep & bucket deposit, h=20

The "clearing sweep" and empty bucket deposition scheme was simplified. C16 cavity GFA=3V, voltage =3.0kV GSRPOS GFA = -4.5V @ injection, sweeps up to +4.5V in 3 ms, and then sweeps down to 0.0V in 3 ms at which time the cavity voltage is reduced to zero. The process is completed in 6 ms. The effect is evident in the two bands of black and white stripes at the bottom of Figure 26. The lower band occurs as the 20th harmonic RF passes through the beam, the intervening grey strip occurs when GSRPOS GFA=+4.5V, and the upper band of stripes indicates the bucket deposition.

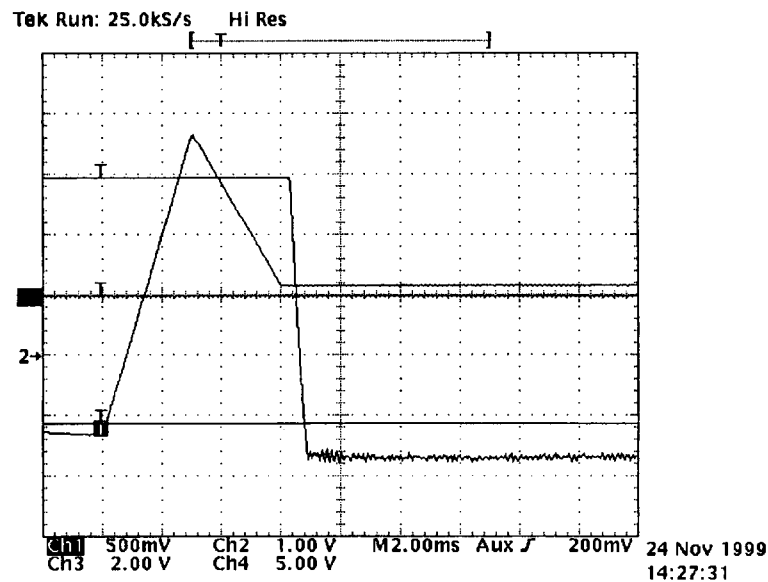


Figure 25: C16 cavity voltage (channel #2 dB) and frequency (channel #3) laws; . RPOS GFA=0.0 volt when the C16 cavity voltage goes to zero.

4.1 1 turn injected, 1.0E12ppp, inject @ C-train= 275ms

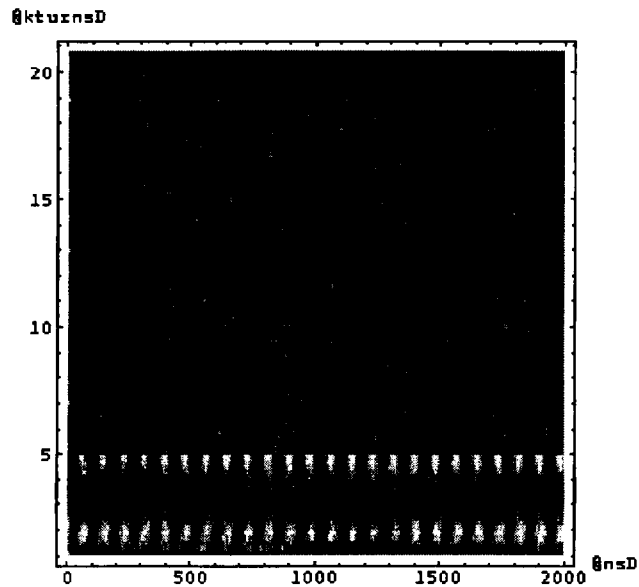


Figure 26: C16 ON, 200 turns/trace, 100 traces, start @ inject, span = 33.3ms, 5 mV/div .

One may obtain a little more contrast by removing the first few profiles which show the last vestiges of h=20 bunched beam.

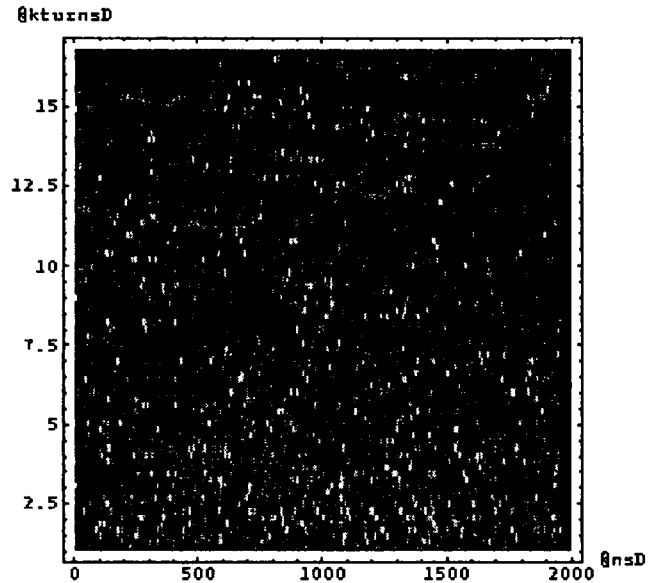


Figure 27: C16 ON, 200 turns/trace, 80 traces, start @ inject+6.7ms, span =26.7 ms, .

The most striking feature of Figure 26 is the absence of h=20 structure. This may be due to the combination of the large momentum spread of the holes (the C16 voltage =3 kV is rather large) and the low beam current.

Date: 24.11.99 Time: 14:29

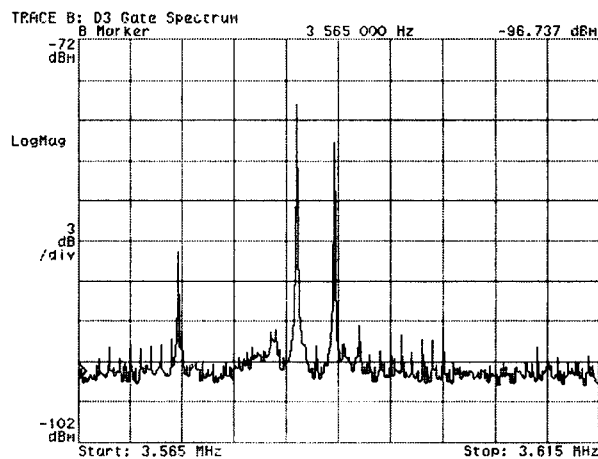


Figure 28: Schottky scan; 1 clearing sweep and deposition; 1 turn injected; .

The scan above is similar to Figure 19 which could indicate that the spikes are due to the bucket deposition.

4.2 2 turns injected, 1.6E12ppp, inject @ C-train= 275ms

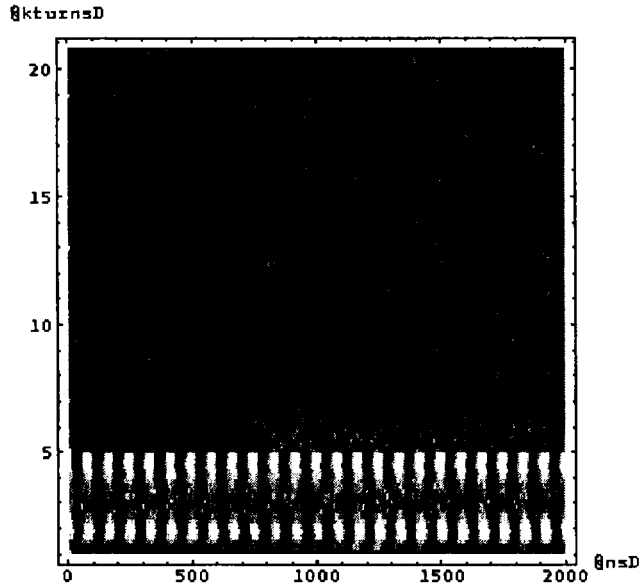


Figure 29: C16 ON, 200 turns/trace, 100 traces, start @ inject, span =33.3 ms, 5mV/div . Harmonic h=1 structure emerges after approx 15 ms has elapsed since injection.

Date: 24.11.99 Time: 14:34

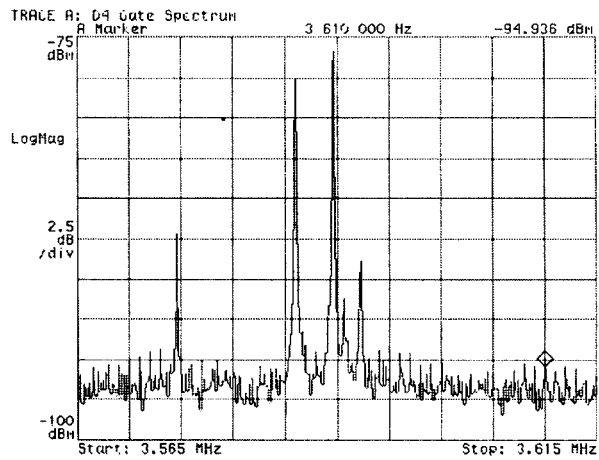


Figure 30 Shottky scan; 1 clearing sweep and deposit, 2 turns injected .

The scan above is similar to Figure 28.

4.3 3 turns injected, 2.4E12ppp, start @ C-train= 275ms

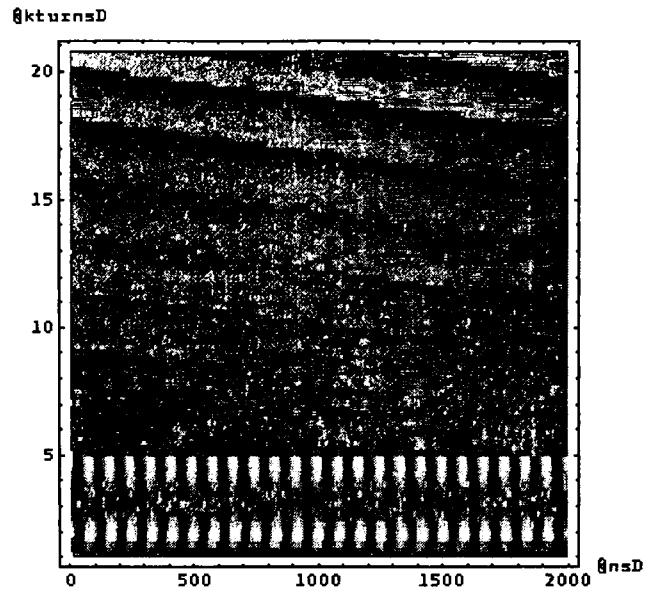


Figure 31: C16 ON, 200 turns/trace, 100 traces, start @ inject, span =33.3ms .

Harmonic h=1 structure is evident and the depth of the modulation increases as time passes. Assuming constancy of the reference RF, the frequency deviation of the h=1 structure seems to diminish as time passes. The value of GSRPOS GFA is 0.0 volt during the acquisition.

Date: 24.11.99 Time: 14:37

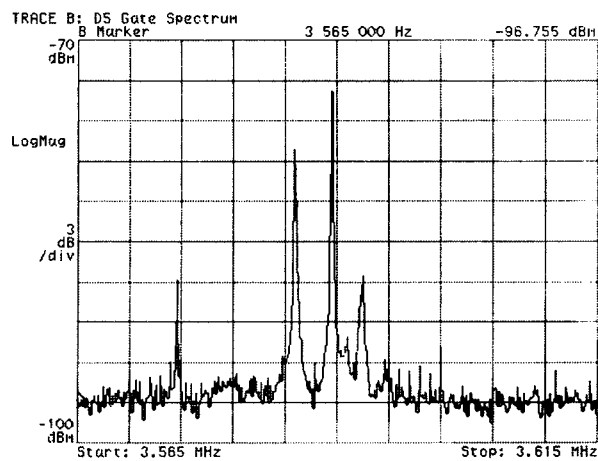


Figure 32: Schottky scan, 1 clearing sweep and deposit, 3 turns injected .

The scan is similar to Figure 30.

4.4 4 turns injected, $3.6E12$ ppp, inject @ C-train= 275ms

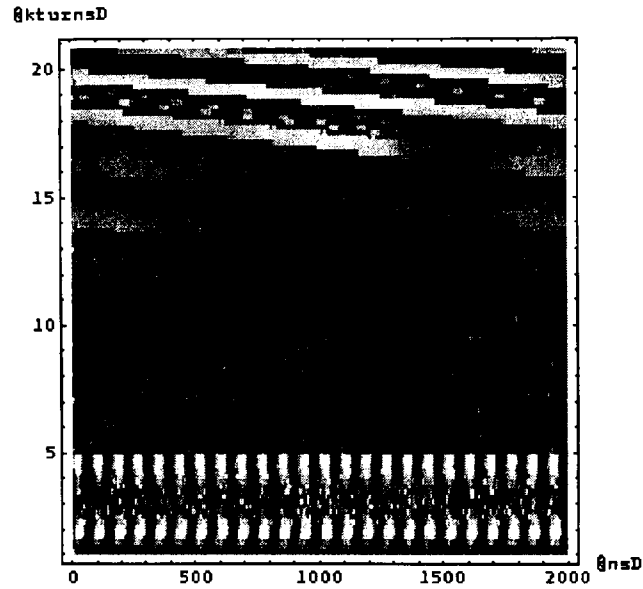


Figure 33: C16 ON, 200 turns/trace, 100 traces, start @ inject, span =33.3ms, 5mV/div . Harmonic h=1 structure is stronger than in the two previous waterfall plots.

Date: 24.11.99 Time: 14:40

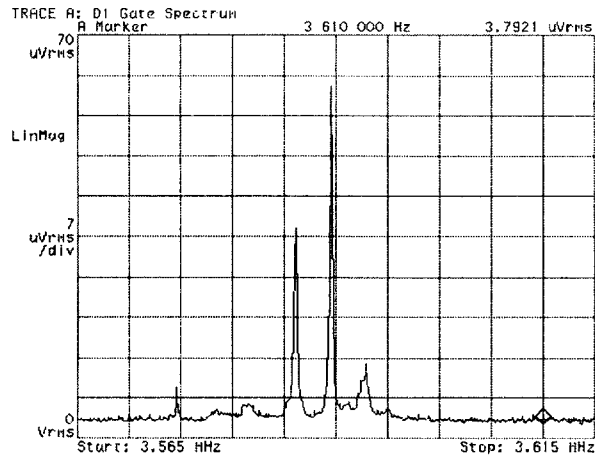


Figure 34: Schottky scan; 1 clearing sweep and deposit, 4 turns injected .

The scan is similar to Figure 32.

4.5 5 turns injected, 5.5E12ppp, inject @ C-train= 275ms

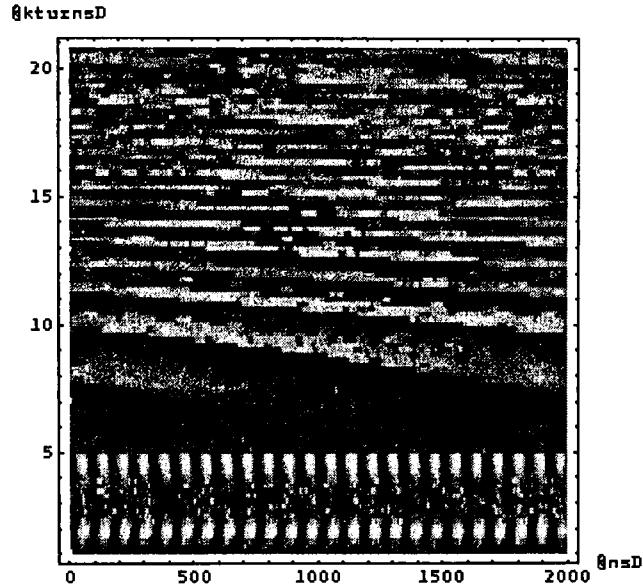


Figure 35: C16 ON, 200 turns/trace, 100 traces, start @ inject, span = 33.3 ms, 20 mV/div, Δf GFA=0.0V at end .

Fourier analysis of each trace/profile initially reveals strong $h=20,40$ harmonics which later disappear while $h=1,2$ components (both stronger than $h=0$) along with weak $h=3,4$ harmonics appear, Figure 36.

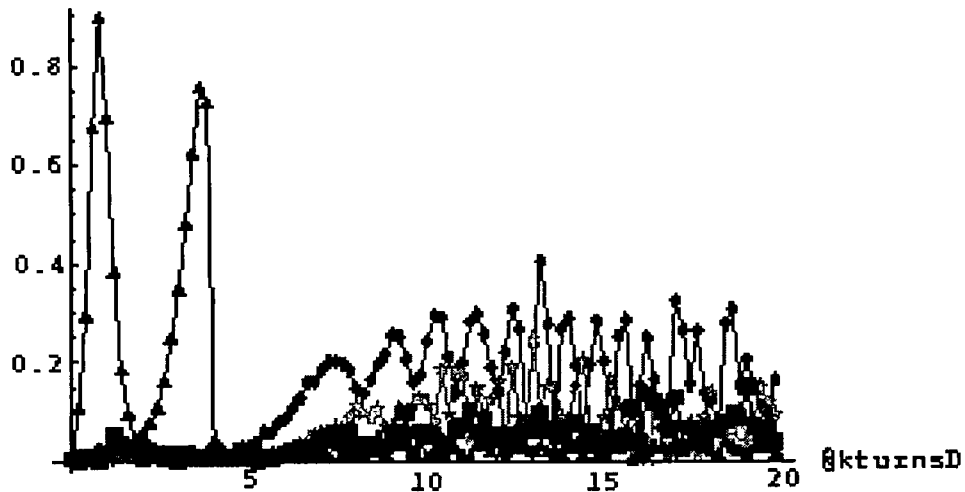


Figure 36: red diamonds $h=1$, green stars $h=2$, blue squares $h=3$, black triangles $h=20$ Fourier components .

The spectrogram is very similar to Figure 40.

Date: 24.11.99 Time: 14:58

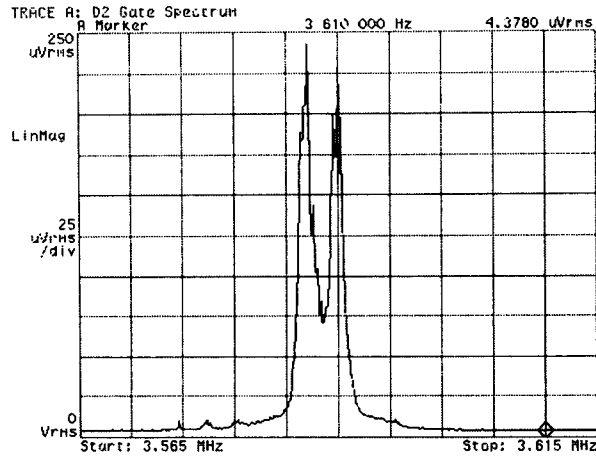


Figure 37: Schottky scan, 1 clearing sweep and deposit, 5 turns injected, .

The scan, Figure 37, looks like the result of a BTFM; and it is tempting to ascribe the notch and two peaks to the empty bucket deposition.

In order to bring the $h=1$ structure to “rest” within the waterfall density plot, GSRPOS was ramped after after the bucket deposition is completed so that the acquisition frequency approximately follows the revolution frequency of the $h=1$ structure. The revised frequency program is idicated below, Figure 38.

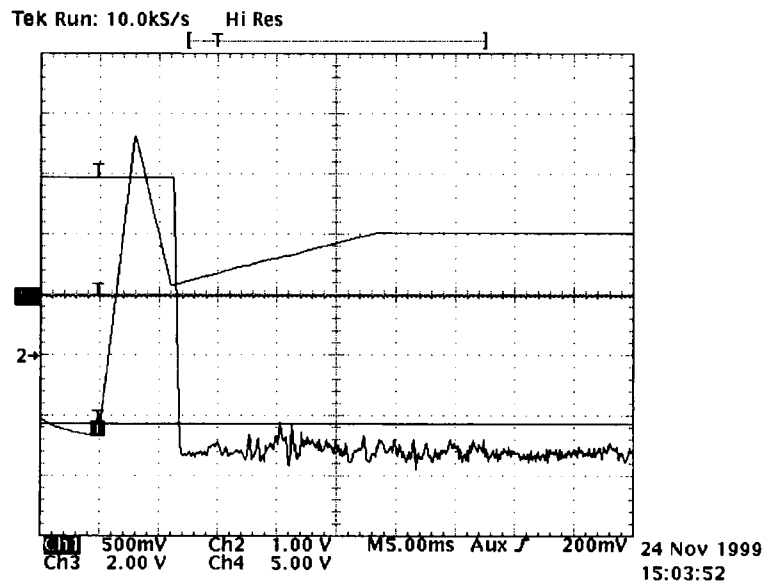


Figure 38: C16 cavity voltage (dB channel #2) and frequency (channel #3) laws .

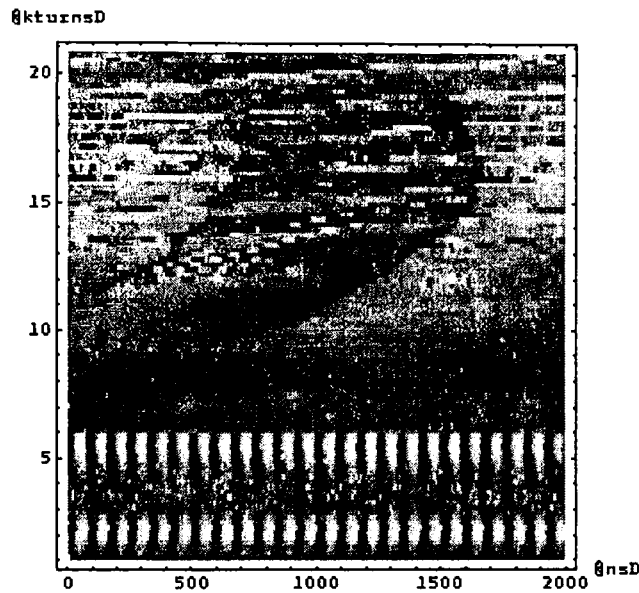


Figure 39: C16 ON, 200 turns/trace, 100 traces, start @ inject, span = 33.3 ms, 20 mV/div, Δf GFA=+1.0V at end, 5 injected turns .

The spectrogram, Figure 40, indicates initial $h=20,40$ harmonics which fade and $h=1,2,3,4$ components which appear afterward.

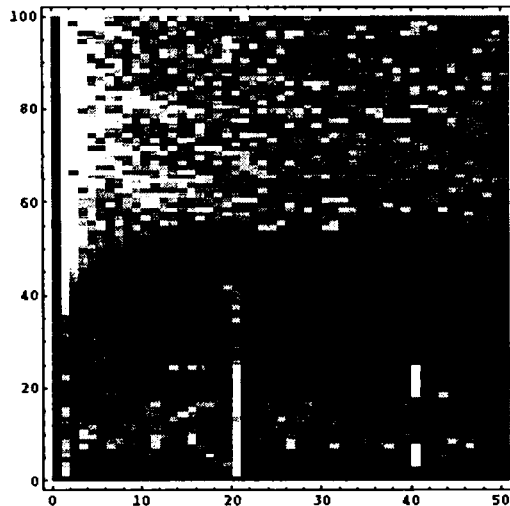


Figure 40: “Spectrogram” or Fourier components (horizontal axis) versus profile number (vertical axis) .

5 C02,C04 OFF; C16 on; Single Clearing Sweep, No bucket deposit

The C16 voltage and frequency program is shown below. Behaviour was measured as a function of the number of injected turns. The waterfall plots, Figure 42 through Figure 47, are very similar as are the Schottky scans, Figure 44 and Figure 46. However, at about 5 injected turns and above, $h=2$ and higher harmonic content appears in the waterfall plots, Figure 49 and Figure 52, and the lower frequency/energy sub-peaks in the Schottky scan become

progressively more prominent, Figure 50 through Figure 55. This could indicate that in addition to space-charge there is an additional impedance producing some collective effect.

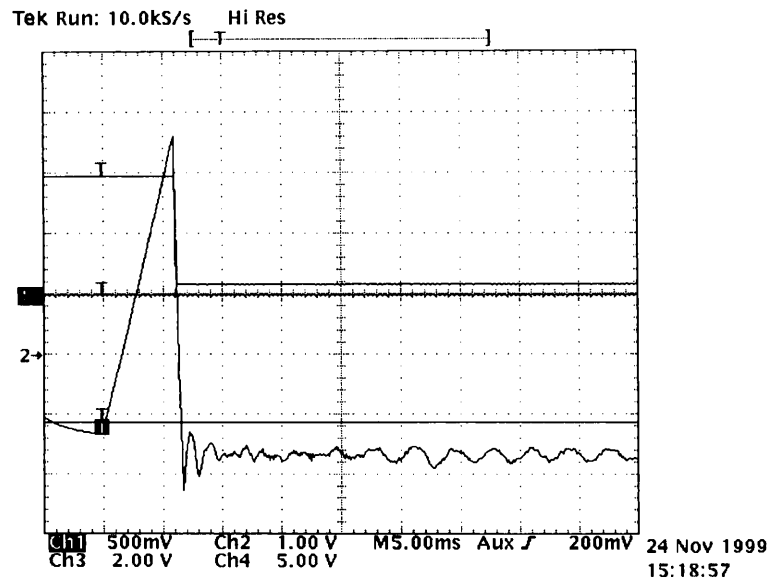


Figure 41: C16 cavity voltage (dB channel #2) and frequency (channel #3) laws .

5.1 2 turns injected, 1.6E12ppp, inject @ C-train= 275ms

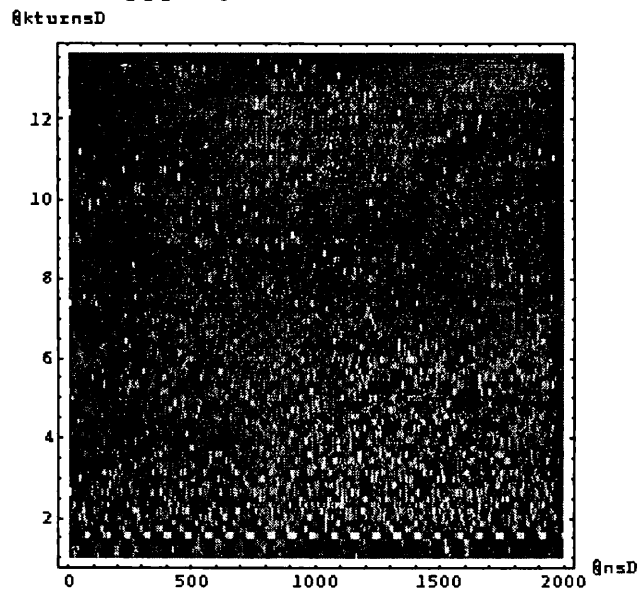


Figure 42: C16 ON, 160 turns/trace, 80 traces, start @ inject+5.3 ms, span =21.3 ms, 5mV/div, .
 "TC16ON42.dat" was bad/corrupted data, and was not used.

5.2 3 turns injected, 2.3E12ppp, start @ C-train= 275ms

@ktuznsD

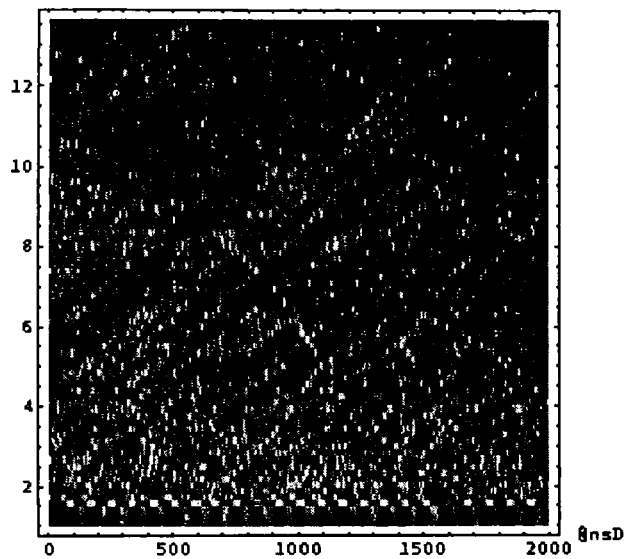


Figure 43: C16 ON, 160 turns/trace, 80 traces, start @ inject+5.3 ms, span =21.3 ms, 2mV/div .

Date: 24.11.99 Time: 15:50

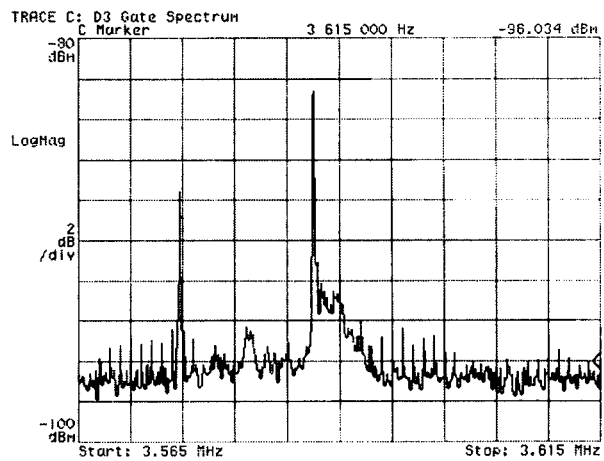


Figure 44: Schottky scan, 1 clearing sweep, no deposit, 3 turns injected .

5.3 4 turns injected, 3.6E12ppp, inject @ C-train= 275ms

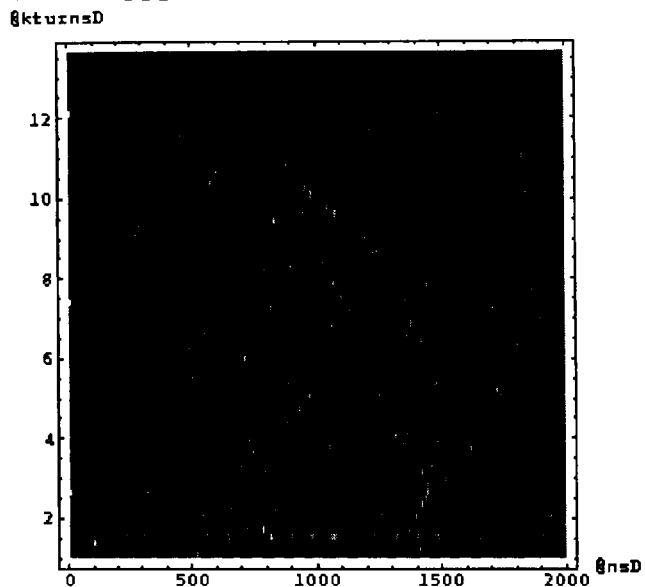


Figure 45: C16 ON, 160 turns/trace, 80 traces, start @ inject+5.3ms, span =21.3 ms, 5mV/div .

Date: 24.11.99 Time: 15:55

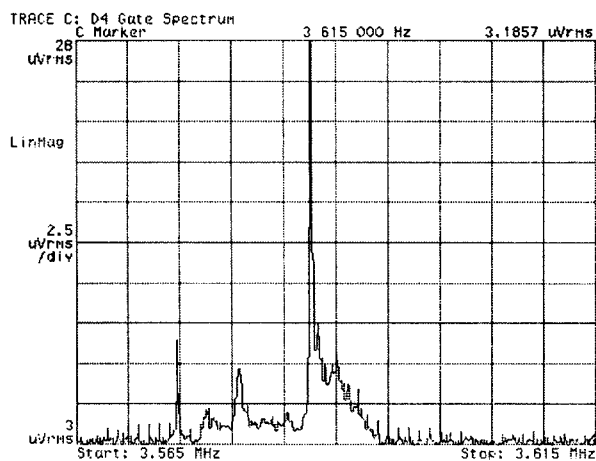


Figure 46: Schottky scan, 1 clearing sweep, no deposit, 4 turns injected .

5.4 5 turns injected, 4.8E12ppp, inject @ C-train= 275ms

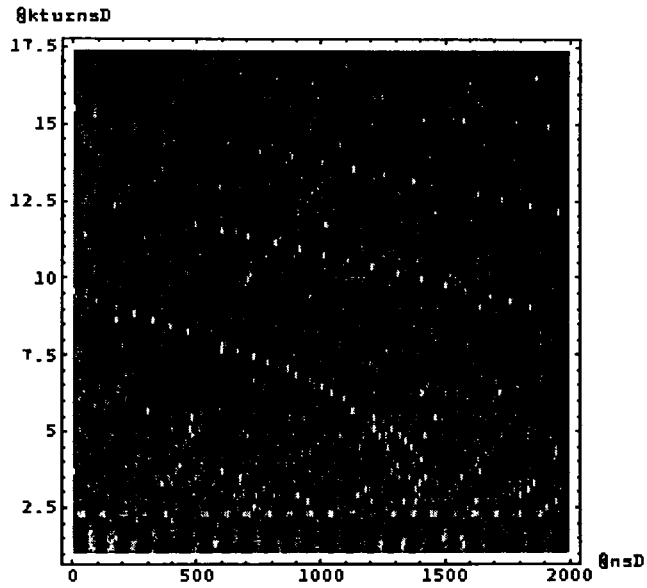


Figure 47: C16 ON, 160 turns/trace, 83 traces, start @ inject+4.5ms, span =22.1ms, 10 mV/div .

Date: 24.11.99 Time: 15:40

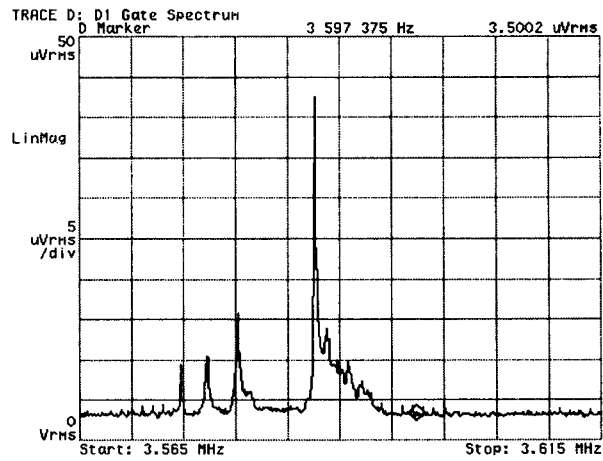


Figure 48: Schottky scan, 1 clearing sweep, no deposit, 5 turns injected .

5.5 6 turns injected, 1.0E12ppp, inject @ C-train= 275ms, h=20

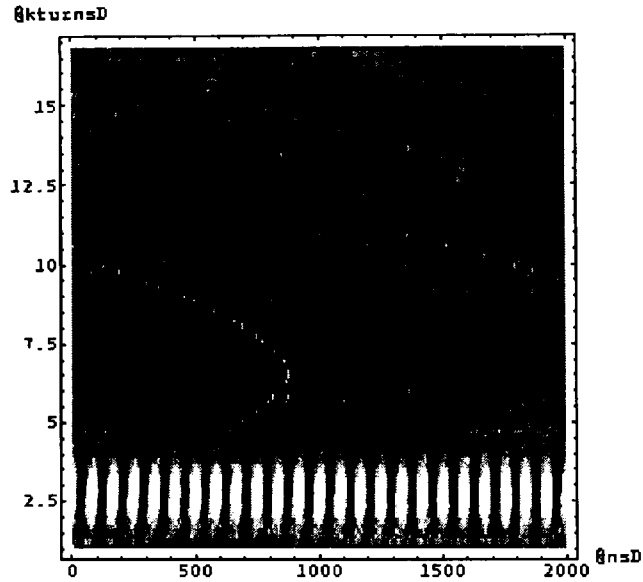


Figure 49: C16 ON, 160 turns/trace, 100 traces, start @ inject, span =26.7ms, 5mV/div .

The spectrogram reveals initial h=20,40 harmonics which quickly fade and very weakly, sporadically growing h=1,2 components along with a very weak h=3 signal.

Date: 24.11.99 Time: 16:00

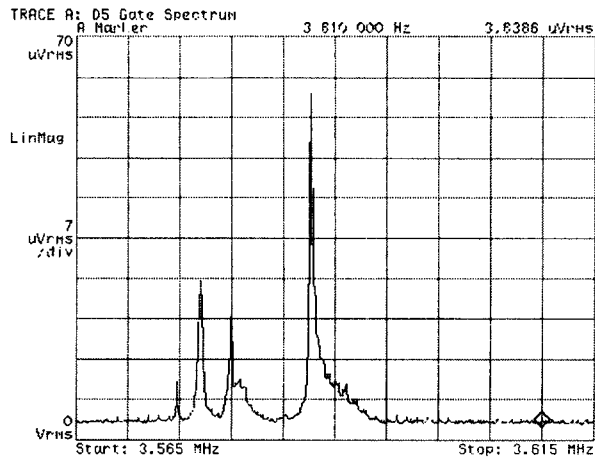


Figure 50: Schottky scan, 1 clearing sweep, no deposit, 6 turns injected .

5.6 7 turns injected, 5.2E12ppp, inject @ C-train= 275ms

Date: 24.11.99 Time: 15:19

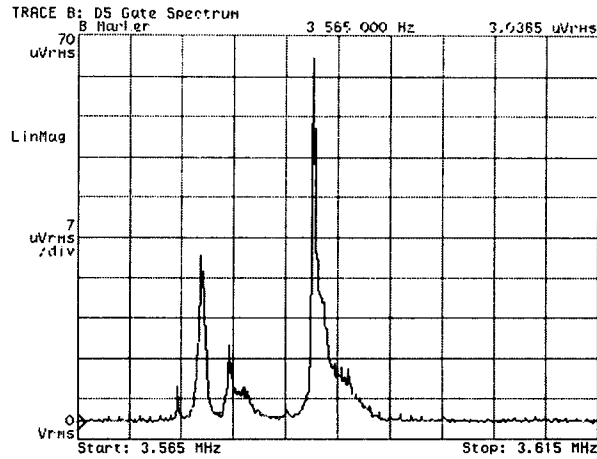


Figure 51: Schottky scan, 1 clearing sweep, no deposit, 7 turns injected .

5.7 10 turns injected, 5.8E12ppp, inject @ C-train= 275ms

#ktuznsD

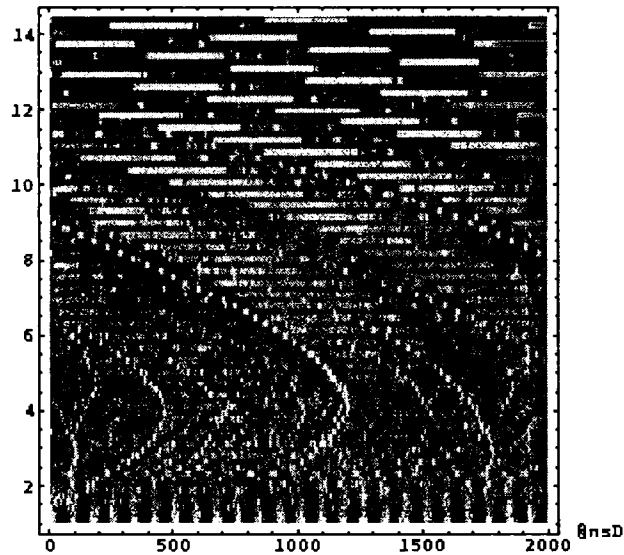


Figure 52: C16 ON, 160 turns/trace, 85 traces, start @ inject+4ms, span =22.7ms, 10 mV/div .

The spectrogram, Figure 53, reveals initial $h=20,40$ harmonics and later weak but growing $h=1,2,3,4$ components with the lower integers growing fastest. From all of the Fourier analyses made (from 24th Nov MD), this is the only case in which there is a very clear growth signature, and this is shown in Figure 54. The Schottky scan, Figure 55, is remarkable in showing a lower energy peak equal in height to the higher energy peak, and we take this as a sign of a coherent instability above threshold intensity.

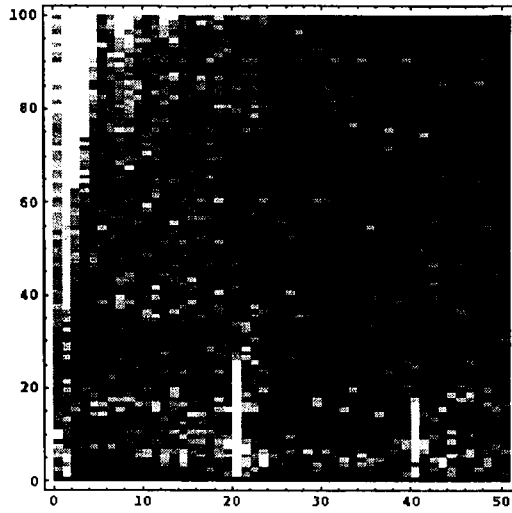


Figure 53: "Spectrogram" or Fourier components (abscissa) versus profile number (ordinate).

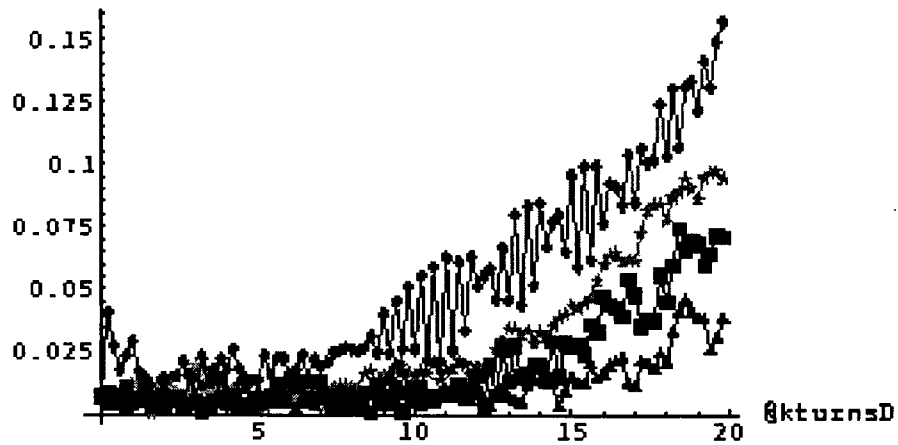


Figure 54: red diamonds $h=1$, green stars $h=2$, blue squares $h=3$, black triangles $h=4$ Fourier components .

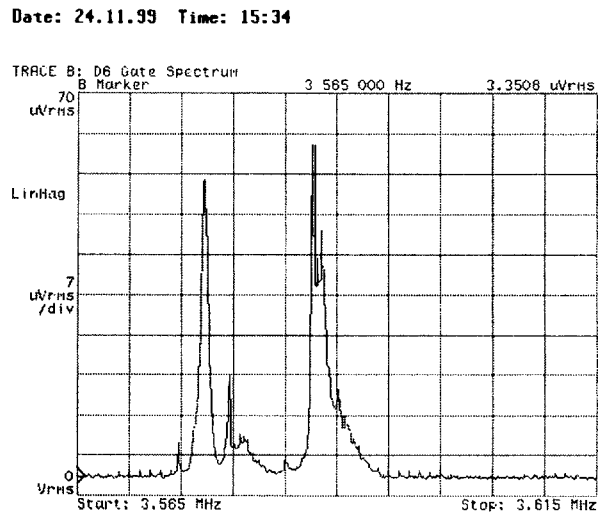


Figure 55: Schottky scan, 1 clearing sweep, no deposit, 10 turns injected .

6 C02,C04 OFF; C16 on; Single Sweep to Centre, h=18

It has been mentioned previously that there was some surprise in not seeing an $h=20$ modulation overwhelmingly clearly after the empty bucket deposition is completed. The most probable explanation is momentum shearing of the relatively wide (in momentum) holes because of the large C16 voltage. However, another possibility could be “memory” of the clearing sweeps. So, as a final simplification, the cleaning sweep was eliminated entirely, and only the empty bucket deposition retained. Duration of the frequency sweep is 6 ms, followed by a gentle ramp (with C16 voltage set to zero) to try and follow the revolution frequency of any beam structure.

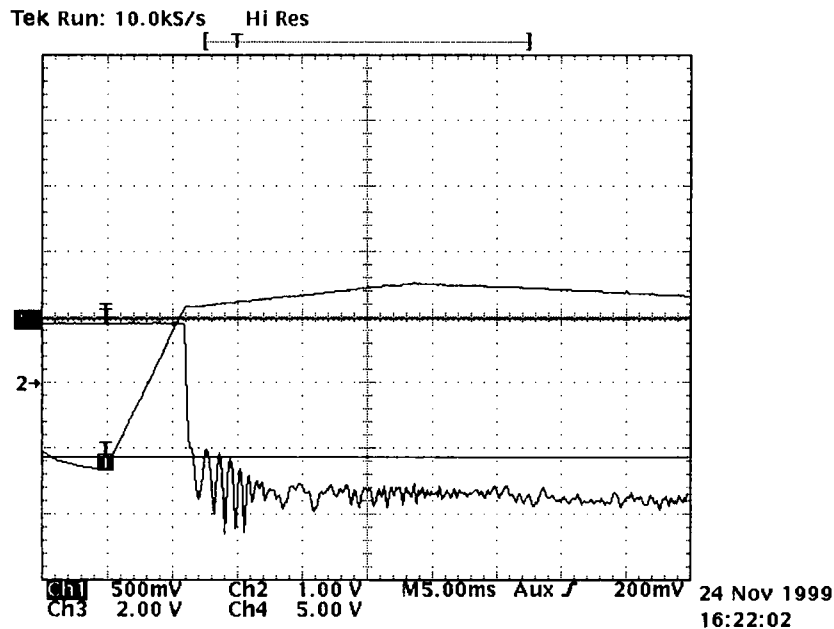


Figure 56: C16 cavity voltage (dB channel #2) and frequency (channel #3) laws .

It was conjectured that holes with large momentum spread (due to the relatively large C16 voltage and the slower frequency ramp) shear quickly and disappear. To test this hypothesis, the C16 voltage was markedly reduced. The harmonic number was also slightly reduced (from $h=20$ to $h=18$) so as to increase the structural resolution; but this is a small effect. Another factor was to use a more sensitive input range for the Tomoscope, and risk some saturation. With the much reduced C16 voltage, one anticipates narrower (in RF phase) and shorter (in MeV) RF buckets, leading to smaller holes. Narrowing the phase-width of the holes enhances space-charge, whereas reducing the momentum with diminishes the shearing effect. The thinner holes are clearly seen in the figures below. The strong contrast in Figure 57 and subsequent “tomoscope” displays is due to saturation of the oscilloscope input levels.

6.1 2 turns injected, C16 GFA=0.95V, VRF=0.3kV, start @ C-train= 279ms

gktuznsD

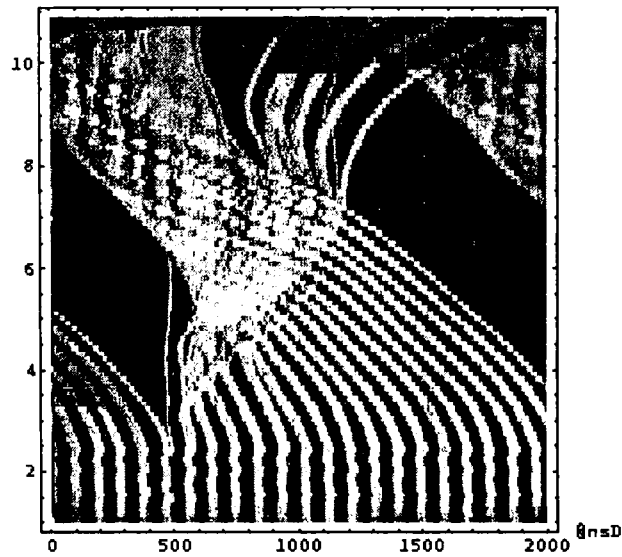


Figure 57: C16 ON, 100 turns/trace, 100 traces, start @ inject+4ms, span =16.7ms, 5 mV/div .

In this particular example, the tendency for $h=18$ holes to shear due to their momentum spread is quite well balanced against the focusing provided by space-charge forces. The spectrogram shows initial $h=18,36$ harmonics which fade and $h=1,2,3$ components (all greater than $h=0$) which vary; all other components are “noise”.

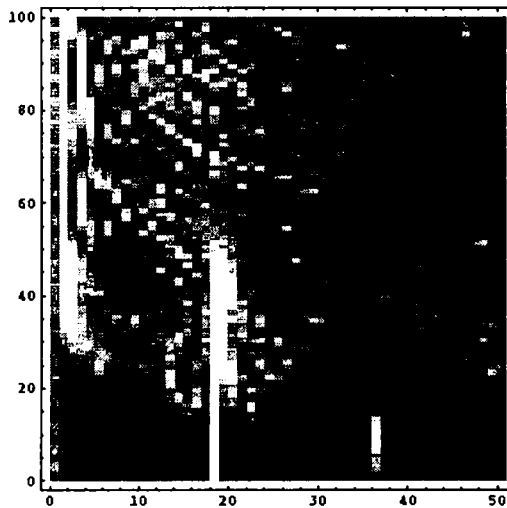


Figure 58: “Spectrograph” or Fourier components versus profile number.

6.2 2 turns injected, C16 GFA=1.50V, VRF=0.55kV, start @ C-train= 279ms

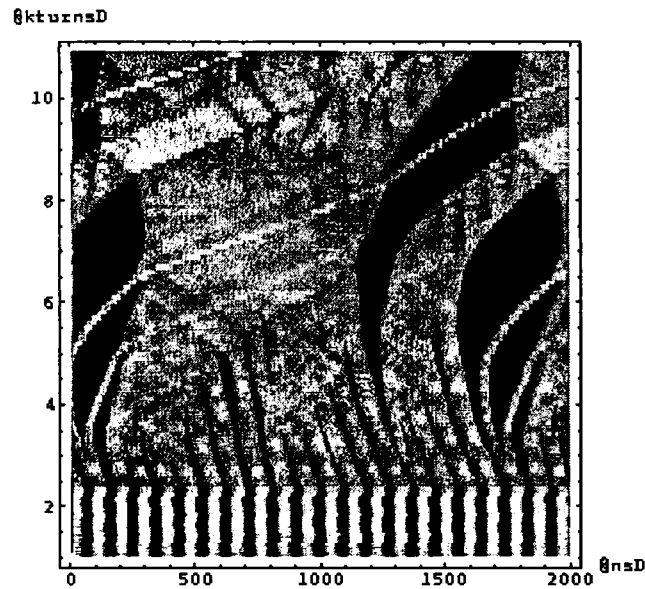


Figure 59: C16 ON, 100 turns/trace, 100 traces, start @ inject+4ms, span =16.7ms .

Increasing the C16 voltage, enlarges the momentum spread and enhances the shearing effect. (compare Figure 57 and Figure 59). The spectrogram shows a clear harmonic-falling of the initial $h=18,36$ harmonics as the modulations debunch, which is accompanied by growth of $h=1,2,3$ components.

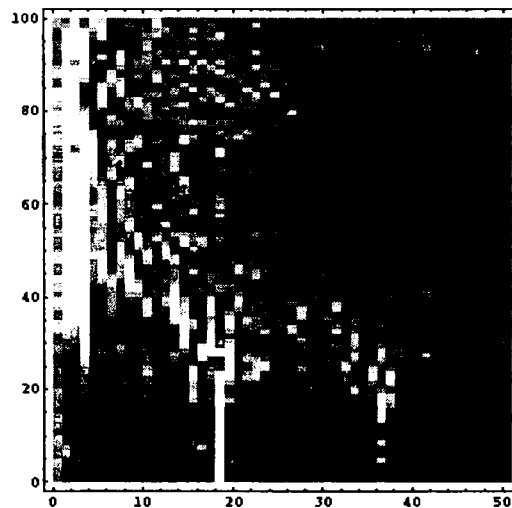


Figure 60: "Spectrogram" or Fourier components versus profile number (100 turns/trace).

6.3 3 turns injected, C16 GFA=1.50V, VRF=0.55kV, start @ C-train= 279ms

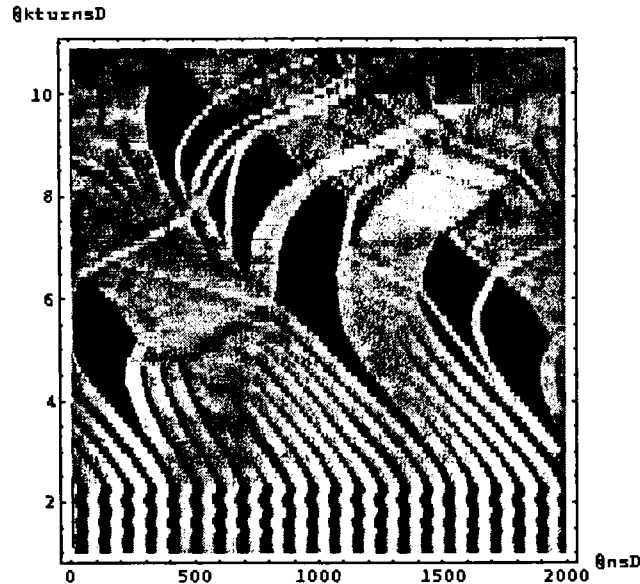


Figure 61: C16 ON, 100 turns/trace, 100 traces, start @ inject+4ms, span =16.7ms, 5 mV/div .

Increasing the beam current, enlarges the space-charge and enhances the focusing effect. (compare Figure 59 and Figure 61). The spectrogram corresponding to Figure 61 shows a less pronounced harmonic-falling than in the previous case.

6.4 4 turns injected, C16 GFA=1.50V, VRF=0.55kV, start @ C-train= 279ms

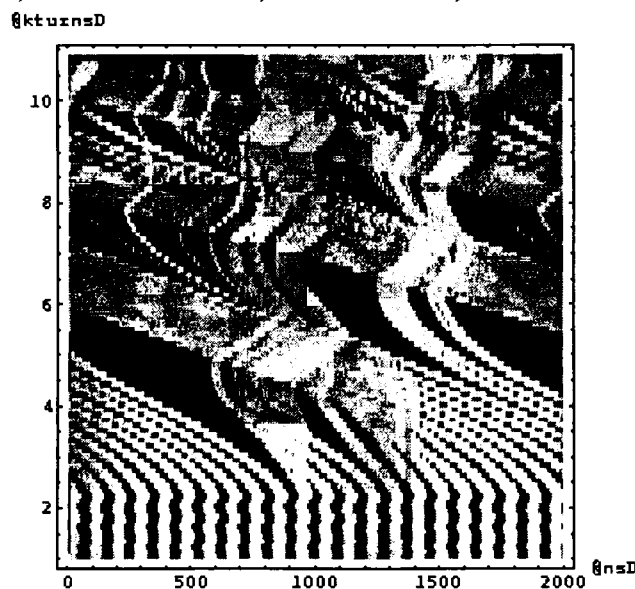


Figure 62: C16 ON, 100 turns/trace, 100 traces, start @ inject+4ms, span =16.7ms, 10mV/div .

Increasing the beam current yet further enhances the space-charge focusing effect leading to even narrower and more self-sustained $h=18$ bunches (compare Figure 59, Figure 61 and Figure 62). The enhanced space-charge also changes the precise energy of the bucket deposit, leading to faster phase slippage. The spectrogram corresponding to Figure 62 shows less harmonic-falling of the initial $h=18,36$ components than in the, which may be interpreted as

the action of space-charge force acting against the tendency to debunch from momentum spread.

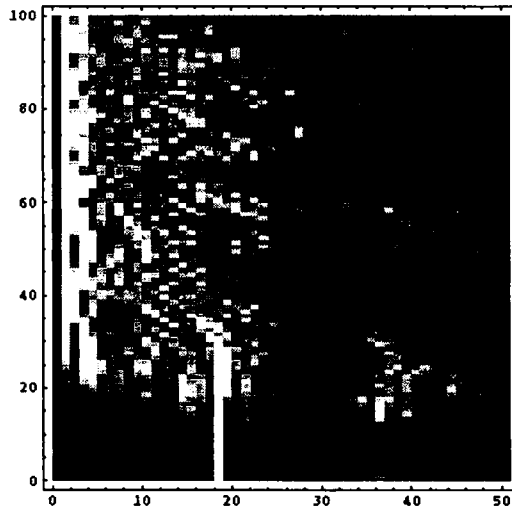


Figure 63: “Spectrogram” or Fourier content versus profile number .

Figure 64 compares the time evolution of the harmonic $h=18$ content of the cases considered in sections 6.1 to 6.4. The faster debunching when the momentum spread of the holes is increased (6.1 versus 6.2) is clearly evident (red versus green curves). The slower debunching that occurs when the intensity is raised (6.2 versus 6.3) is evident from a comparison of the green and blue curves. The harmonic content in each case was normalized by its initial strength.

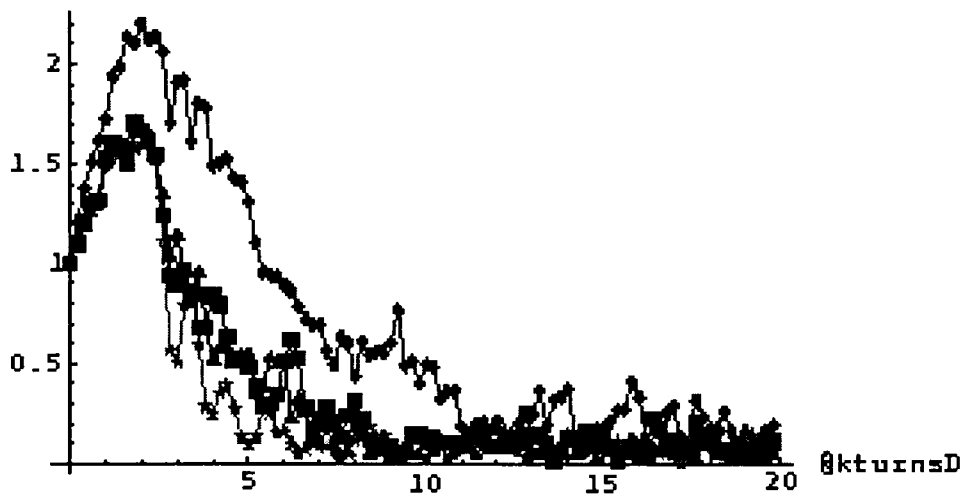


Figure 64: red diamonds = case 6.1, green stars = case 6.2, blue squares = case 6.3, black triangles = case 6.4 .

7 Conclusion

Firstly, post-processing the turn-by-turn profile data with “Mathematica” has given unequivocal evidence for “injection bubbles” and their surprising longevity. There is also evidence that some of the voids are “linac bubbles” with width about 10 ns. Adjusting the reference frequency for data acquisition does help to make the “tomoscope” plots less confusing.

Secondly, coherent signals present in the Schottky scan does make interpretation of these (ostensibly incoherent) spectra problematic; and this serves as a caveat for all inferences made below. In particular, the coherent signals may be orders of magnitude larger than the incoherent and swamp the frequency spectrum.

Empty bucket deposition certainly does affect the outcome of the scan. Whenever high harmonic buckets are deposited (sections 3.1, 4.1—4.5), we always see two close spikes (separation ≈ 0.045 MHz @ $h=6$); whereas with C16 off (section 2) or just clearing sweeps (sections 3.2 and 5) there is a single central spike. Whether the deposit is preceded by three sweeps (section 3.1) or by one (section 4.2-4.3), the spectrum is the same. In all cases (C16 off or on), there is a low-energy signal spike ≈ 0.15 MHz (@ $h=6$) below the main peak (or peaks). This low energy spike is more evident when there is no bucket deposit, and its prominence increases with beam intensity (section 5).

When there is no bucket deposition, we may compare the case C16 off (section 2.2—2.4) with that of one clearing sweep (section 5.2—5.4), where there is little difference between the Schottky scans excepting for a slight skewness in the latter case, or compare against 3 sweeps (section 3.2) where the Schottky scan is visibly broadened.

Evidence from this MD and others (17th and 22nd November 1999) points to there being two collective effects at work: firstly, there is space charge whose effect is simply proportional to intensity; secondly, there is some undiagnosed coasting beam instability, with threshold of about 6 injected turns, which confuses the beam observations. Given the growth of low ($h=2,3,4$) but not high harmonics, a likely candidate for the offending impedance is the C02 and C04 RF systems.

Diagnosing the precise nature of collision between holes is not possible without the beam momentum spectrum; instead one must make inferences based on a single projection of the phase space ensemble. From the line density, it appears that in the majority of cases, collision between holes does not leads to coalescing – rather that they are glancing collisions. However, there are also several ambiguous cases where the outcome of collision could be either coalescing or a debunching that gives the appearance of hole merging.